The Chemical Composition of Fine Ambient Aerosol Particles in the Beijing Area

Bettina Nekat, Dominik van Pinxteren, Yoshiteru Iinuma, Thomas Gnauk, Konrad Müller and Hartmut Herrmann

Leibniz-Institute for Tropospheric Research, Permoserstr. 15, 04318 Leipzig, Germany
nekat@tropos.de

INTRODUCTION

China suffers significantly from increased particle emissions due to the rapid economic growth during the last decades.This aerosol can influence local air quality and visibility as well as cloud formation processes by serving as Cloud Condensation Nuclei (CCN). Their chemical composition affects the microphysical and optical properties of the clouds such as hygroscopic growth or droplet activation. The Hachi-project (Haze in China) aims to investigate this relation and to identify possible particle sources. Therefore an extended chemical analysis of the submicron airborne particles especially of the organic fraction is performed.

Measurement site

Wuqing National Ordinary Meteorological Observing Station

39°23'8.53"N
117°1'25.88"E

Fig. 1: The measurement site was located at the Wuqing National Ordinary Meteorological Observing Station, China, a background site which is situated between the megacities Beijing (northwest) and Tianjin (southeast).

Sample collection

Winter campaign: 01/03/ – 04/04/2009
Summer campaign: 13/07/ – 13/08/2009

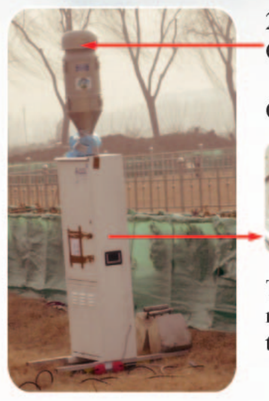

24 hours system
Cut-off 1 µm ($Dp_{aerodynamic}$)

Quartz fibre filters

Sample number
Winter: 34
Summer: 33
Total: 67

Transport from measurement site back to the institute in deep-frozen state.

Fig. 2: The DIGITEL DHA-80 High Volume sampler with the PM_1-inlet on the top.

Chemical analysis

The filters were analyzed for particle mass concentration, (1) carbonaceous material and inorganic constitutes, (2) small polar water-soluble organic compounds, (3) non polar water-insoluble organic compounds and (4) surface active substances.

EC, OC, WSOC
Inorganic ions
.

Anhydromono- and monosaccharides, Sugar alcohols and Dicarboxylic acids

PAHs
Hopanes
n-Alkanes
.

Saturated and unsaturated n-fatty acids

Fig. 3: The DIGITEL quartz fibre filter from the 02/03/2009.

RESULTS

1 PM_1 mass concentration

The average PM_1 concentration for the winter and summer campaign differ in total mass concentration (Tab. 1) as well as chemical composition (Fig. 4).

Table 1. The range and mean of mass concentrations for winter and summer campaign in µg/m³.

	Minimum - Maximum	Mean
Winter	20.4 – 121.9	53.8 ± 26.8
Summer	12.8 – 65.7	36.8 ± 13.4

The highest PM_1 mass concentration was observed from prevailing southern wind directions during winter time (Fig. 5a), but during summer time no prevailing wind direction was noted (Fig. 5b).

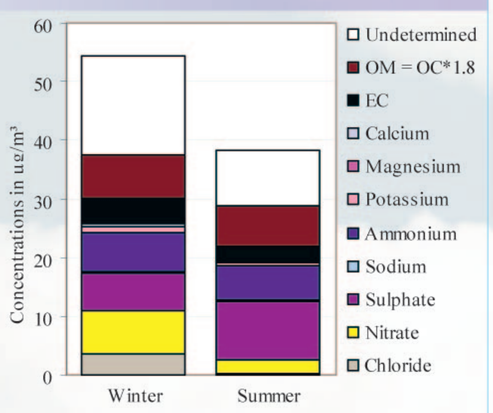

Fig. 4: The campaign average concentrations of the main constitutes in µg/m³ for both measurement periods.

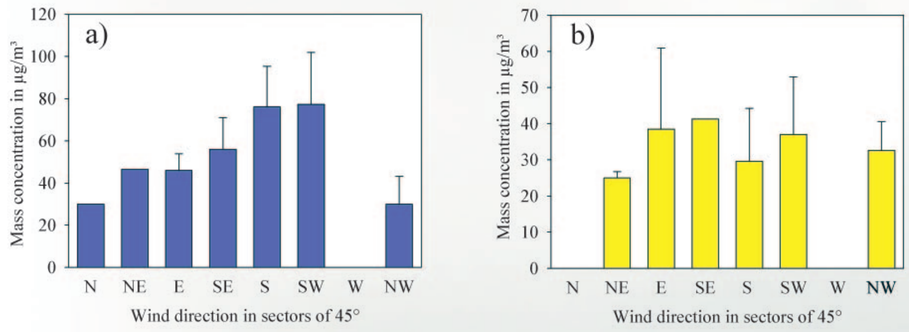

Fig. 5: The PM_1 mass concentrations in µg/m³ of the a) winter and b) summer campaigns averaged for 8 wind direction sectors of 45° (N: 337.6-22.5°, NE: 22.6-67.5°, E: 67.6-112.5°, SE: 112.6-157.5°, S: 157.6-202.5°, SW: 202.6-247.5°, W: 247.6-292.5°, NW: 292.6-337.5°).

2 Biogenic emission

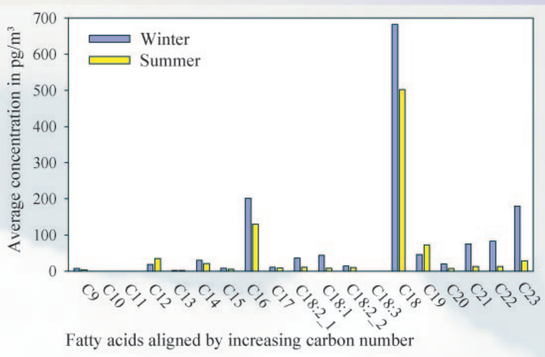

C9 n-nonanoic acid
C18:1 ≡ 9-(Z)-octadecenoic acid
C18:2_1 ≡ 9,12-(Z,Z)-octadidecenoic
C18:2_2 ≡ 9,12-(E,E)-octadidecenoic
C18:3 ≡ 9,12,15-(E,E,E)-octatridece-noic acid

Fig. 6: The average concentration of 19 saturated and unsaturated fatty acids (FA) for the winter and summer campaigns in pg/m³. The C18 and C16 saturated n-fatty acids are the dominant fatty acids during both measurement periods and are mostly of microbiological origin.

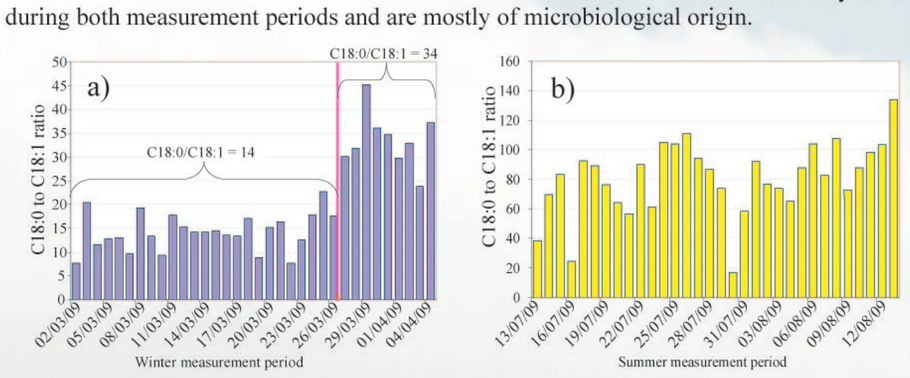

Fig. 7: The C18:0 to C18:1 ratio serves as an processed aerosol indicator, because the unsaturated FA breaks down much faster than the saturated homologue. During a) the winter campaign two different periods are observed. For b) the summer period no such effect was observed.

3 Seasalt emission

The highest chloride and sodium concentrations during the summer time are observed from prevailing eastern wind direction (Fig. 8). This may imply a direct inflow from the sea and a possible marine influence. For the winter campaign no such effect was observed.

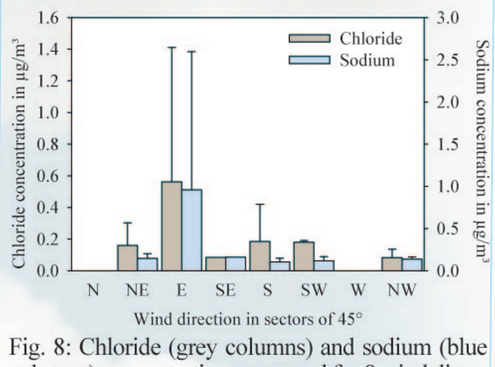

Fig. 8: Chloride (grey columns) and sodium (blue columns) concentrations averaged for 8 wind direction sectors of 45°.

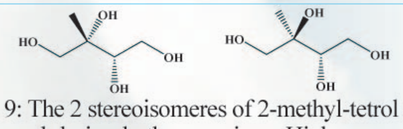

Fig. 9: The 2 stereoisomeres of 2-methyl-tetrol are observed during both campaigns. Higher concentrations were observed during the summer period. They are known as isoprene oxidation products and their primary emission is negligible.

4 Traffic emission

Hopanes and EC are anthropogenically emitted from the combustion of fossil fuel. PAHs are emitted from different sources. As can be seen from Fig. 10 and the correlation coefficient in Table 2, engine combustion might be a source of PAHs.

Table 2: Correlation coeffients of vehicle exhaust originated from potential traffic originated compounds.

		Σ of PAHs	EC
Winter	Σ of hopanes	0.9229	0.7443
Summer	Σ of hopanes	0.3815	0.4539

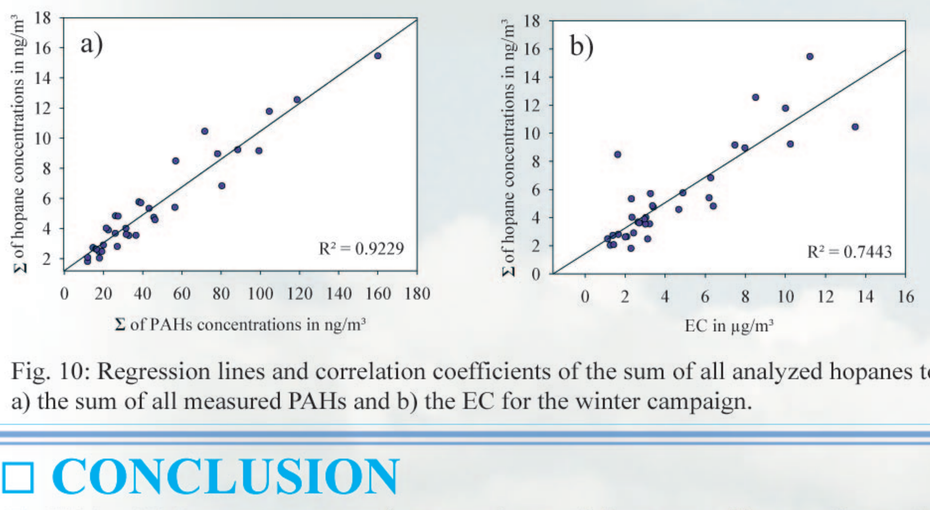

Fig. 10: Regression lines and correlation coefficients of the sum of all analyzed hopanes to a) the sum of all measured PAHs and b) the EC for the winter campaign.

5 Biomass burning emission

The anhydromonosaccharide levoglucosan is known as a biomass burning tracer and was detected as the most abundant saccharide during both campaigns. The PAH retene is often found in biomass burning particles originated from conifers (Li et al., 2009, Simoneit 1999), which was identified only during the winter measurements. Apparently both compounds are not originated from the same sources (Fig. 11, 12). This suggests more sources for levoglucosan than just the combustion of conifers. Another possible source is the biomass burning of grass related plants as indicated by the ion ratios in Table 3.

Table 3: Ion ratios for biomass burning indication

	Chloride/Potassium	Chloride/Ammonium	PM
Engling et al., 2009	2 – 3 (Rice straw)	1.1	2.5
Iinuma et al., 2007	6 (Savannah Grass)	3.4	1
This Study	4	0.6	1

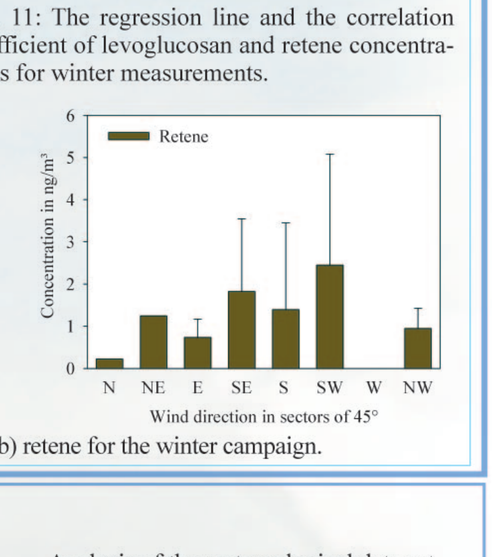

Fig. 11: The regression line and the correlation coefficient of levoglucosan and retene concentrations for winter measurements.

a)

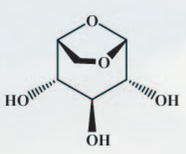

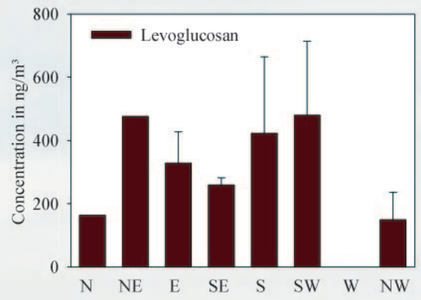

b)

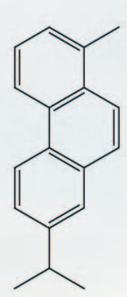

Fig. 12: The chemical structures and mass concentration distributions of a) levoglucosan and b) retene for the winter campaign.

CONCLUSION

- Higher PM_1 mass concentrations are observed from prevailing southern wind direction during the winter time.
- Microbiological as well as BVOC emissions during the summer time are observed. During the winter measurement two periods of different processed aerosol was detected.
- During the summer time a marine influence was detected.
- Traffic is suggested to be an important emission source during the winter and summer campaign as well as biomass burning.
- More than one kind of emission sources are possible.

OUTLOOK

Chemical analysis of the time- and size-resolved particle samples from the 11-stage Berner impactor.

Carbon sum parameter

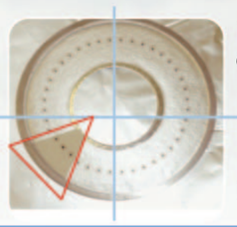

Water soluble organic carbon

Metals

Main ions

Analysis of the meteorological data set (temperature, relative humidity and wind speed).

Analysis of the air mass origin with the mesoscale WRF model.

PMF analysis of the complete chemical/meteorological data set.

Literature

Li, Z.; Porter, E. N.; Sjödin, A.; Needham, L. L.; Lee, S.; Russell, A. G.; Mulholland, J. A. Atmospheric Environment 2009, 43, 4187-4193
Simoneit, B. R. T. Environ. Sci. Pollut. Res. 1999, 6, 159-169
Engling, G.; Lee, J. J.; Tsai, Y. W.; Lung, S. C. C.; Chou, C. C. K.; Chan, C. Y. Aerosol Sci. Technol. 2009, 43, 662-672
Iinuma, Y.; Brüggemann, E.; Gnauk, T.; Müller, K.; Andreae, M. O.; Helas, G.; Parmar, R.; Herrmann, H. J. Geophys. Res. 2007, 112, D08209

Acknowledgement

This work is supported by the German Science Foundation under grant number DFG WI 1449/14-1 and by the National Natural Science Foundation of China (NSFC) under grant No. 40875001.